Measurement of Soil Resistivity in Order to Determine the Buried Walls Trajectory

Mihai Stelian MUNTEANU[1], Levente CZUMBIL[1], Dan Doru MICU[1], Stefan Florin BRAICU[1], Sorin NEMETI[2], Mariana PISLARU[3]
[1]*Technical University of Cluj-Napoca, Cluj-Napoca, 400114, Romania*
[2]*Hisotry and Philosophy Faculty, Babes-Bolyai University, Cluj-Napoca, 400084, Romania*
[3]*Hisotry Museum, Turda, 401154, Romania*
mihai.munteanu@ethm.utcluj.ro

***Abstract*—The importance of archaeometric investigations, performed with technical support is not only that eases the work of archaeologists, but also contributes to optimize human, financial and time resources. Thus the study highlights the results of investigation of an archaeological site from the imperial roman era through a method specific to electrical engineering. Accordingly, based on some soil resistivity measurements made in the Legionary Camp of *Potaissa* - fortress where the 5th Macedonian Legion camped, members of the Archaeometry Laboratory from the Technical University of Cluj-Napoca were able to identify and establish the trajectory of buried walls that were marking the specific construction of the barracks belonging to the troops in *Cohors I Miliaria*. In order to perform this task, a genetic algorithm based technique was used to determine the different soil layers.**

***Index Terms*—soil properties, geophysical measurements, electrical resistance measurements, genetic algorithms, object detection.**

I. Introduction

A. The Legionary Castrum from Potaissa (Turda)

On the occasion of Marcomanic wars the emperor Marcus Aurelius transferred in Dacia the 5th legion Macedonica, establishing its garrison at Potaissa (today Turda, Cluj County). The camp that the Legion has built at Potaissa worked for about a century (approx. 170÷270 AD.), until Emperor Aurelian (270-275 AD.), this being one of the approximately 70 legionary camps of the Roman Empire. The best analogy in size (573 x 408 m, 23.37 ha) and planimetry are obviously other legionnaire forts built during the reign of Marcus Aurelius (Locic in Pannonia Superior and Albing in Noricum) [1], [2], [3].

Fort ruins were seen on Citadel Hill until the nineteenth century, attracting the attention of travellers and collectors of antiques, such as Pierre Lescalopier, Csipkés Elek, Orbán Balasz, Karl Torma or Téglás István.

The archaeological research of the building itself started after mid-twentieth century when, in 1958, with the occasion of some public utility works, Ion Horatiu Crisan conducted a survey in the southeast corner of the fort. Then systematic archaeological research led by Acad. Mihai Bărbulescu are conducted continuously from 1971 up to now. These targeted fortification elements (inside the bastion of the north-western corner of the fort) and the west gate (*porta Decumani*). Inside the fort, there were exhaustively investigated the headquarters (*principia*) building with a surface of 0.89 ha, and the baths, that were the largest in the Dacia province, stretching on a surface of 0.64 ha. Also there were partially investigated cohort barracks *miliaria of some cohortes quingenariae* and granary (*horreum*). Other studies have considered the camp roads, their connection to the road system in the Dacia province and the water supply of the fortress [4], [5], [6].

B. The Legionary Castrum from Potaissa (Turda)

Identification and demarcation of the barracks planimetry from *Cohors I Miliaria* occurred during the archaeological research, in the campaigns of 1990-1992. Through section A/1990, facing northwest/southeast in *latus praetorii dextrum* of the fort of the 5th legion Macedonica, barracks I-IV have been surprised, disposed parallel with the headquarters building. Barracks were divided into *contubernia* as researched walls are arranged thereon, and between the barracks I-II and III-IV were identified access driveways (bounded by a layer of alluvial gravel) that communicates directly the *via principalis*. The most detailed has been researched barrack IV that consists of 12 *contubernia*, bordered by a portico to barrack III. During the research in 2011, it was completed the planimetry of *Cohors I Miliaria*.

Figure 1. Section *S01/2011*, barrack IV, *Cohort I Miliaria*, Potaissa

Fig. 1 presents archaeological research section S01/2011 (barrack IV) from *Cohort I Miliaria* (Dimensions: 3 x 10 m; Orientation: North-South, drawn at north of the barrack IV next to room C). The earth stratification at research site was:

1. *Modern Humus* (0÷0.20 m depth);
2. *Medieval-Modern Debris level* (0.20÷0.35 m depth) black loosen earth with tegular material (tiles, bricks), stone etc.
3. *Habitation level* (0.35÷0.55 m) defined by compacted yellowish-gray soil, which is submission to the Roman period within the chamber A. Between 7.20 m and 7.65 m,

Digital Object Identifier 10.4316/AECE.2017.01015

the Roman habitation level is cut by a modern pit (0.50 m deep).

4. *Black earth*, archaeological sterile (0.55÷0.70 m).

5. At 8.25 m in sterile ground a mortar lens defines (0.60÷0.65 m depth), that is the level of wall construction.

Through section S01/2011, squares 5-10 was partially uncovered the inside of a barrack (room A and room B) and two interiors of *contubernia* from barrack III. The southern wall of the barrack, oriented east-west, has a thickness of approx. 0.50/0.60 m and is built in *opus incertum* from Sandulesti limestone. A height of 0.50 m it is kept (three rows of stone). Partition wall with an irregular route and 0.50 m wide, is built of limestone with mortar, having tegular fragments too, right at the base (reused material).

In the room A were found Roman pottery, iron and bronze objects, glass, pieces of military equipment and a bronze coin issued four Legionnaire banners issued by Nicaea (obverse illegible). A parallelepiped form column (dimensions: 0.85 x 0.57 x 0.30 m), placed on a bed of crushed limestone, was found in this section at 2.85 m from the south wall of the chambers A and B. This indicates the existence of the porch on the southern side of the barrack III. The opening the porch was 10 *pedes*. There were found several fragments of limestone column spindles, probably Podeni, and other archaeological materials: a fragmentary *mortarium*, glass and tegular material.

In order to ease the work of archaeologists, the members of the Archaeometry Laboratory from the Technical University of Cluj-Napoca have applied and tested a truly electrical engineering specific method to determine the trajectory of buried walls. Soil resistivity measurements have been carried out at *Cohors I Miliaria*, Potaissa archaeological site to identify variations in earth electrical resistivity and thus to detect the presence of buried ancient constructions (see Fig. 2). This method could significantly reduce financial, human and time resources needed for archaeologic sites research and to increase the probability of archaeological findings.

Figure 2. On site soil resistivity measurements at Cohort I Miliaria

II. Soil Resistivity Measurements

A. Applied Wenner four Point Method

Usually, to determine the soil resistivity the galvanic contact between an array of electrodes and the earth is used, as in the case of the Dipole-Dipole, Wenner or the Schlumberger array methods [7, 8].

The Wenner Four Point methos, is the most frequently used soil resistivity measurement method in electrical engineering applications. This techniques has the advantage that the spacing between the voltage electrodes (***P1&P2***) increases in the same as the spacing between the current electrodes (***C1 & C2***), therefore less sensitive equipment are required for deep earth measurements.

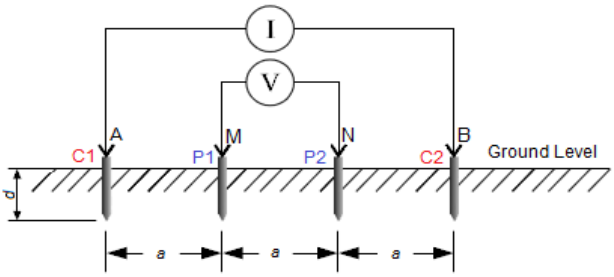

Figure 3. Wenner's four probe method

For the Wenner Four Point method (see Fig. 3), the current (***C1&C2***) and voltage (***P1&P2***) electrodes are placed in a straight line, with equal spacing. In Fig. 3 ***a*** is the distance between two adjacent electrodes, ***d*** is current electrodes length and ***I*** is the injected d.c. current.

During the measurements the test equipment injects a d.c. current, ***I***, into the earth via the outer two electrodes (the current ***C1&C2*** electrodes). The current flows through the earth (considered as resistive material) and generates a potential difference between the inner two, voltage electrodes. Using Ohms law, the testing equipment displays the apparent soil resistance in [Ω] for a given electrode spacing (i.e. ***R=V/I***).

Considering the earth as a uniform, homogeneous and isotropic half-space (from now on, all "uniform" structures will be considered as homogenous and isotropic), the potential field generated by the Wenner electrode array can be computed and this way to relate the soil resistivity to the electrode array geometry [9-11]:

$$V = U_{P1} - U_{P2} = \frac{\rho \cdot I}{2\pi}\left[\frac{1}{C1P1} - \frac{1}{C2P1} + \frac{1}{C2P2} - \frac{1}{C1P1}\right] \quad (1)$$

where U_{P1} and U_{P2} are potentials of the two voltage electrodes (***P1&P2***), ***C1P1*** is the distance between electrode ***C1*** and ***P1***, etc.

The quantity inside the brackets depends on the actual distance between the electrodes, whether or not they are placed on a straight line. Denoting this quantity with ***1/K*** equation (1) could be rewritten as:

$$V = \frac{\rho \cdot I}{K} \quad (2)$$

where ***K*** is a geometric coefficient, and for the Wenner Four Point method is equal to $K=2\cdot\pi\cdot a$.

Therefore, the apparent soil resistivity for a specific earth depth, ***a***, could be determined from the measured voltage ***V*** and the injected current ***I*** considering the same, ***a***, horizontal spacing between the electrodes [8].

$$\rho_a(a) = 2 \cdot \pi \cdot a \cdot \frac{V}{I} \quad (3)$$

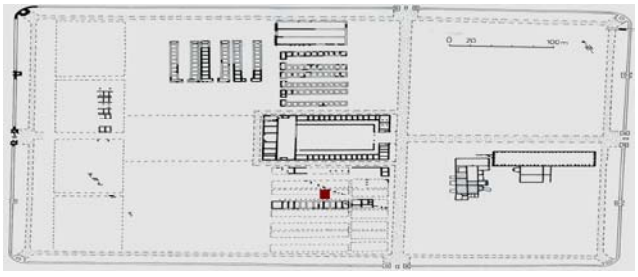

Figure 4. *Potaissa camp planography (investigated area is marked in red)*

B. On site Soil Resistivity Measurements

The soil resistivity measurements carried out by the Archaeometry Laboratory have focused on an area of the barrack IV of *Cohors I Milliaria* (see Fig. 4).

On-site technical investigations aimed to identify buried walls routes, and thus to validate their presence in the camp planography, where "intuited" trajectories are drawn in dotted line (see Fig. 4). Therefore, the soil resistivity measurements were performed at several points above a presumed chamber, considering a 1 m distance between each measurement point as in Fig. 5 is showed:

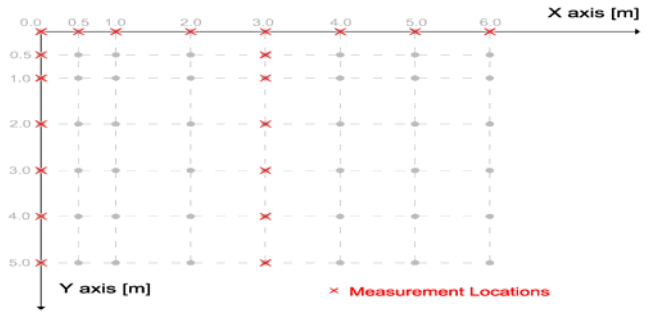

Figure 5. Grid map of soil resistivity measurement locations

At each measurement location, the apparent soil resistivity was determined for different depths: 20 cm, 60 cm, 100 cm and 150 cm. Apparent soil resistivity variation along investigation grid map X axis (were a buried wall is intuited) and Y axis (no wall is intuited) for each measurement depth are presented in Fig. 6÷9:

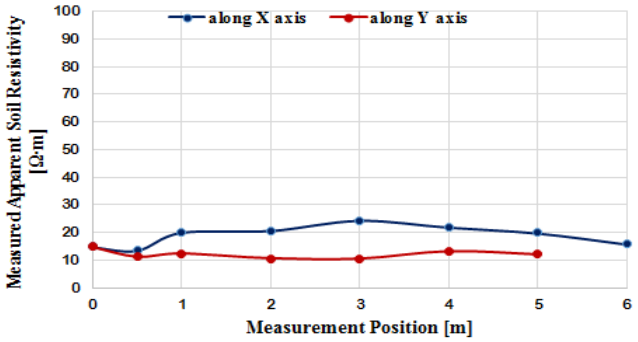

Figure 6. Apparent soil resistivity at a depth of 20 cm

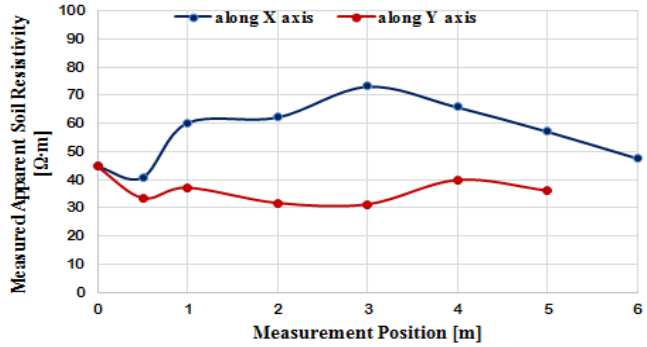

Figure 7. Apparent soil resistivity at a depth of 60 cm

Looking to the apparent soil resistivity variation, along *X* axis (above the intuited wall), it is noted that the investigated soil resistivity has a high value at a depth of 60 cm and 100 cm, and a low value at the depth of 20 cm and 150 cm. This result is interpreted by the fact that the ancient stone wall detected (probably located at a depth ranging somewhere between 50 cm and 120 cm) lead to changes in measured resistivity; consequently, there is a sharp increase in its characteristic from the level of earth above the wall (values between 10 Ω·m and 15 Ω·m) to higher values, ranging between 45 Ω·m and 70 Ω·m. Along the *Y* axis (across the intuited chamber) the apparent soil resistivity is relatively constant for each measurement depth with a value between 10 Ω·m and 30 Ω·m (see Fig. 6÷9).

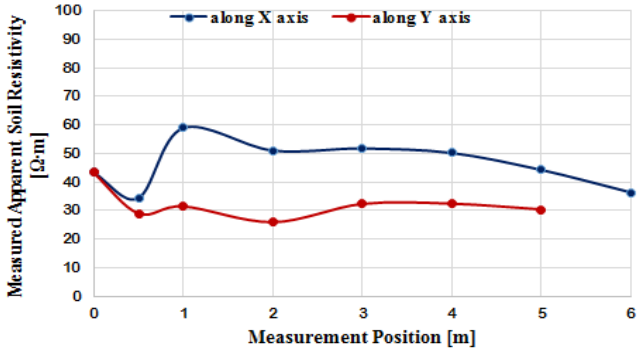

Figure 8. Apparent soil resistivity at a depth of 100 cm

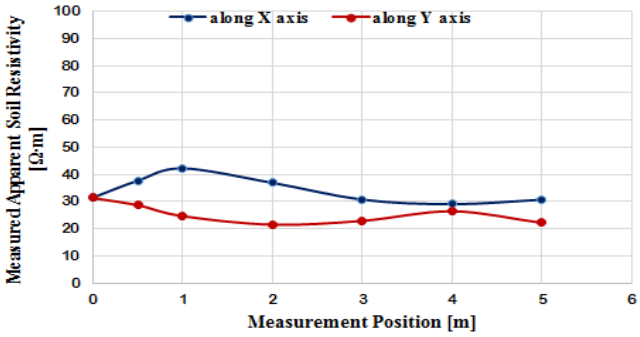

Figure 9. Apparent soil resistivity at a depth of 150 cm

The results of the last set of measurements (at a depth of 150 cm, along X axis) reveal again a low apparent soil resistivity value, located around 35 Ω·m (see Fig. 9). This value, less than the corresponding depths with the wall (60 cm and 100 cm), but higher than in the shallow depths, free of construction (20 cm), can be explained by the fact that the determined apparent soil resistivity value is considered for the entire ground volume, up to the depth of 150 cm, which implicitly contains the wall located at a smaller depth.

III. Multi-Layer Soil Structure Determination

In order to determine the trajectory of the detected underground ancient constructions from the measured apparent soil resistivity values the equivalent horizontal multi-layer soil structure has to be computed for each measurement point.

A. Applied Genetic Algorithm Optimization Method

To obtain the proper equivalent horizontally layered earth structure in accordance with measured apparent resistivity data, the authors have previously developed a genetic algorithm based optimization technique [12]. With the implemented Genetic Algorithm (GA), the optimum earth layer thickness and resistivity are determined. Similar artificial intelligence approaches have been presented in [13, 14].

The implemented iterative GA search process starts with an initial randomly generated population formed by 30

individuals representing possible multi-layer soil model solutions. The chromosome encoding of a GA solution contains the thickness and resistivity values of each soil layer scaled to the [0÷1] range:

$$C = \{\rho_1, h_1, \rho_2, h_2, \ldots, \rho_L\} \quad (4)$$

Each possible horizontally layered soil model is evaluated based on the mean square error between the measured Wenner apparent resistivity values and the computed apparent resistivity curve:

$$MSQ_{Err} = \frac{1}{N}\sum_{i=1}^{N}[\rho_a(a_i) - \rho_{Ea}(a_i)]^2 \quad (5)$$

where MSQ_{Err} denotes the mean square error; N is the number of earth resistivity measurements; $\rho_a(a_i)$ is the measured Wenner apparent resistivity for an electrode spacing a_i and $\rho_{Ea}(a_i)$ is computed based on the following relationships [15-20]:

$$\rho_{Ea}(a) = \rho_1[1 + 2F_L(a) - F_L(2a)] \quad (6)$$

where:

$$F_L(a) = 2a\int_0^{\infty}\frac{K_{L1}e^{-2\lambda h_1}}{1 - K_{L1}e^{-2\lambda h_1}}J_o(\lambda a)d\lambda \quad (7)$$

with $J_0(\lambda a)$ – the zero order first kind Bessel function [12];

$$K_{L1} = \frac{k_1 + K_{L2}e^{-2\lambda h_2}}{1 - k_1 K_{L2}e^{-2\lambda h_2}},\ K_{Lj} = \frac{k_j + K_{Lj+1}e^{-2\lambda h_{j+1}}}{1 - k_j K_{Lj+1}e^{-2\lambda h_{j+1}}} \quad (8)$$

$K_{LL-1}=k_{L-1}$; L – the number of horizontal earth layers; h_j – layer j thickness and k_j – the reflection factor between soil resistivity layer j and layer $j+1$:

$$k_j = \frac{\rho_{j+1} - \rho_j}{\rho_{j+1} + \rho_j} \quad (9)$$

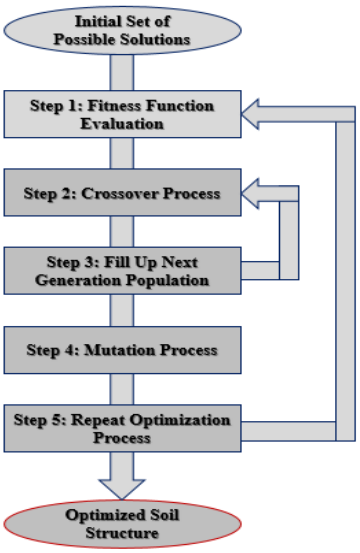

Figure 10. Implemented Genetic Algorithm optimization process.

To identify the equivalent optimum horizontal multi-layer soil structure, the GA starting population is trained into an iterative process, presented in Fig. 10 and described by the following steps:

Step 1*: All the possible soil model solution from current GA population are evaluated and the best 5 solutions are selected for the next iteration (next GA generation).*

Step 2: *Two possible soil model solutions are randomly selected as "parents" of a crossover process to get two new solutions for the next GA generation.*

During the crossover process from the selected two "parent" solutions 6 new solutions are generated. The first two "children" soil models are obtained by applying an arithmetical crossover operator [9]:

$$\begin{aligned} C_1^t &= \alpha \cdot P_1^t + (1-\alpha)\cdot P_2^t \\ C_2^t &= \alpha \cdot P_2^t + (1-\alpha)\cdot P_1^t \end{aligned} \quad (10)$$

where t represents the t^{th} parameter of an multi-layer soil model; C_n and P_m represents the n^{th} "child" and m^{th} "parent" soil model solution; α is a randomly generated scaling factor (between 0 and 1).

Two other possible solutions are generated besed on a max-min crossover operator [13]:

$$\begin{aligned} C_3^t &= \min(P_1^t, P_2^t) \\ C_4^t &= \max(P_1^t, P_2^t) \end{aligned} \quad (11)$$

while the final two "children" GA solutions are obtained using a classical one-point crossover operator [14]:

$$\begin{aligned} C_5 &= \left(P_1^1 \quad \cdots \quad P_1^k \quad P_2^{k+1} \quad \cdots \quad P_2^r\right) \\ C_6 &= \left(P_2^1 \quad \cdots \quad P_2^k \quad P_1^{k+1} \quad \cdots \quad P_1^r\right) \end{aligned} \quad (12)$$

with k a randomly selected crossing point.

Based on the evaluated mean square error values the best two "children" soil model solutions are selected and pased to the next GA generation population.

Step 3: *Step 2 is repeated until the new GA population will have the same number of possible earth structure solutions as the current GA population.*

Step 4: *Four randomly selected GA solutions are subjected to a mutation GA operator.*

For each parameter of the four GA solutions selected for the mutation process probability test is applied. If the probability test is passed than an arithmetical parameter value alteration is carried out:

$$C^t = C^t + (0.5 - \alpha)\cdot M \quad (13)$$

where α is a randomly selected value from the 0÷1 range, and M is a predefined mutation coefficient.

Step 5: *Go to the next iteration (next GA generation) and start over Step 1.*

The above described iterative GA optimization process is repeated 2000 times or until the mean square error for the best solution is smaller than a previously imposed value. This way the implemented GA optimization technique identifies the proper parameter values for a specific horizontally layered soil model. Similar ar

B. Obtained Multi-Layer Soil Structures

In order to identify buried walls and constructions trajectory the earth stratigraphy for each measurement point was reconstructed based on measured apparent soil resistivity values and using the above presented genetic algorithm.

TABLE I. DETERMINED SOIL STRUCTURE AT FIRST MEASUREMENT POINT (0 M , 0 M)

Layer No.	Layer Resistivity [Ω·m]	Layer Thickness [m]	Reflection Coefficient [p.u.]
1	14.92	0.18	-1
2	185.36	0.37	0.928
3	7.58	Infinite	-0.922

The obtained horizontal multi-layer soil structure for the first measurement point along *X* axis (where underground walls belonging to barrack IV were intuited) are presented in Table I and Fig. 11 respectively.

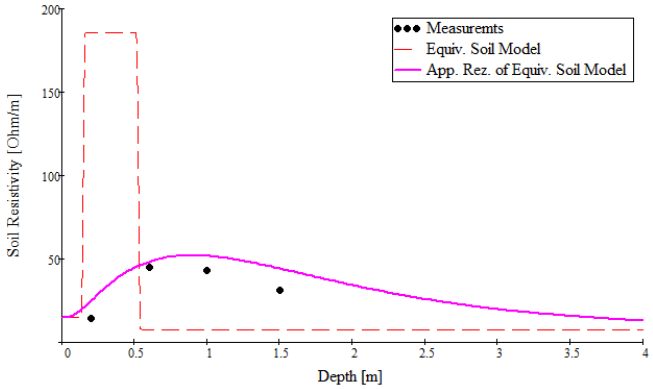

Figure 11. Determined soil structure at first measurement point (0,0)

Fig. 11 clearly show the presence of ancient walls remains at a 0.2 m depth (an approximately 40 cm thick layer with a considerably higher resistivity, 185 Ω·m).

Determining the soil stratigraphy at each measurement point, variations in underground constructions structure could be detected (gaps, door places, wider walls, etc.). Table II presents the measured apparent soil resistivity values for measurement point 2 m along X axis while the corresponding horizontal multi-layer structure are indicated in Fig. 12 and Table III respectively:

TABLE II. MEASURED SOIL RESISTIVITY AT MEASUREMENT POINT 2 M ALONG X AXIS

Depth	0.2 m	0.6 m	100 m	150 m
Measured Apparent Resistivity	20.73 Ω·m	62.20 Ω·m	51.08 Ω·m	36.94 Ω·m

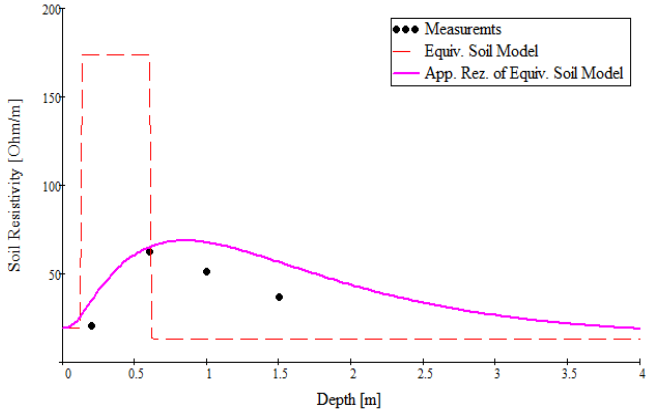

Figure 12. Determined soil structure at measurement point 2 m along *X* axis

TABLE III. DETERMINED SOIL STRUCTURE AT MEASUREMENT POINT 2 M ALONG X AXIS

Layer No.	**Layer Resistivity [Ω·m]**	**Layer Thickness [m]**	**Reflection Coefficient [p.u.]**
1	19.48	0.15	-1
2	173.56	0.48	0.886
3	12.88	Infinite	-0.832

The second part of the study focused on analyzing measured apparent soil resistivity values and corresponding soil stratigraphy within the enclosure of a chamber, to identify its delimitation. Table IV presents measured apparent soil resistivity values at measurement point (3 m, 2 m), which should be the middle of one of barrack IV chambers.

TABLE IV. MEASURED SOIL RESISTIVITY AT MEASUREMENT POINT (3 M, 2 M)

Depth	0.2 m	0.6 m	100 m	150 m
Measured Apparent Resistivity	10.44 Ω·m	31.32 Ω·m	32.35 Ω·m	22.99 Ω·m

As it was expected, applying the implemented genetic algorithm, a uniform soil structure with an equivalent 28 Ω·m resistivity was obtained (see Fig. 13):

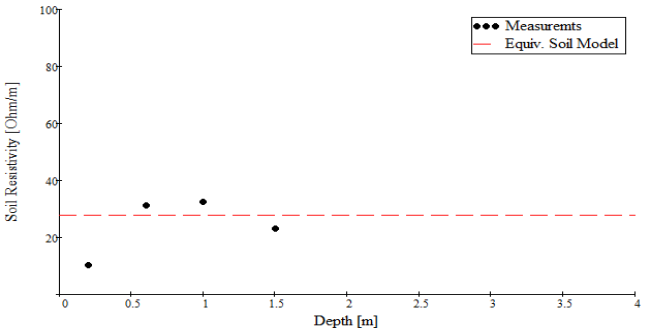

Figure 13. Determined soil structure at measurement point (3 m, 2 m)

Measured apparent soil resistivity values for measurement points corresponding to the middle of a chamber showed that at a depth of 100 cm, 150 cm and 200 cm, the soil resistivity is approximately the same, and at a shallower depth (60 cm), it does not vary significantly, indicating no structures other than the soil (stone, brick, tile), as expected.

The resistivity value measured at a shallow depth (20 cm) was not taken into account because of several residues in the study area, stones and tiles at the surface of the soil and in close proximity to the surface. Therefore, to improve the accuracy of measurements, it is recommended that previously investigated surface to be cleaned of any material which could induce errors.

IV. CONCLUSION

Investigations in the field of archaeometry are complex, the extent of which is enhanced by the interdisciplinary character of research: conjugation with the electric engineering items related to the history. Thus, the convergence of scientific rigor in both areas, we are looking for accession to remarkable results in archeology by conducting preliminary technical measurement.

The soil electric resistivity measurements have succeeded to evidence the path of some buried walls, marking the specific construction of the barracks belonging to the troops in *Cohors I Miliaria*.

In this way, it has been highlighted the possibility of using the electrical engineering in archaeological study, an idea that can lead to exceptional results through which archeology do a qualitative, fundamental leap: engineering investigations will allow the transition from the classical, empirical approach, to the one based in advance on a technical "diagnostic" of the target area. A genetic algorithm approach has been implemented to identify the presence of underground buried walls based on soil resistivity

measurements. An archaeometric study will preface proper archaeological excavations and the results will be on MATTER: excavations will be made punctually in the areas where ruins are indicated by technical means, thus achieving optimization in the use of human, time and financial resources.

According to the protocols signed between Technical University of Cluj-Napoca (Laboratory of Archaeometry), Babes-Bolyai University, Cluj-Napoca and the town hall of Turda (the History Museum of Turda), the use of this method will be extended in the perimeter of the 5th Macedonian Legion *Castrum* from *Potaissa*, in order to identify other structures - typical to military and civilian construction - from the imperial epoch.

REFERENCES

[1] M. Barbulescu, "Din istoria militară a Daciei romane. Legiunea V Macedonica şi castrul de la Potaissa, Ed. Dacia, pp. 5-200, 1987

[2] C. Barbulescu, "Arhitectura militară şi tehnica de construcţie la romani. Castrul de la Potaissa", pp. 5-99, Ed. Napoca Star, 2004

[3] M. Barbulescu, Mormântul princiar germanic de la Turda (Das germanische Fürstengrab von Turda), pp.7-380, Ed. Tribuna, 2008

[4] M. Pislaru, "The Roman Coins from Potaissa. Legionary Fortress and Ancient Town", pp. 25-150, Ed. Mega, 2009

[5] M. Barbulescu, "Inscripţiile din Castrul Legionar de la Potaissa (The Inscriptions of the Legionary Fortress at Potaissa)", pp. 5-280, Ed. Academiei Române, 2012

[6] M. Barbulescu, A. Cătinaş, C. Luca, A. Husar, P. Huszarik, M. Grec, C. Barbulescu, "The Baths of the Legionary Fortress at Potaissa", Proc. of the 17th International Congress of Roman Frontier Studies, Ed. Limes, pp. 431-441, 1999

[7] G. Papaiz-Garbini, L. Pichon, M. Cucchiaro, "Multilayer ground determination from apparent resistivities and impact on grounding resistances", in Proc. of the 2014 International Symposium on Electromagnetic Compatibility, Tokyo (EMC'14/Tokyo), Tokyo, Japan, May 12-16, 2014, online: http://www.ieice.org/proceedings/EMC14/contents/pdf/16P2-B5.pdf

[8] R. D. Southey, M. Siahrang, S. Fortin, F. P. Dawalibi, "Using Fall-of-Potential Measurements to Improve Deep Soil Resistivity Estimates" , IEEE Transactions on Industry Applications, vol. 51, no. 6, pp. 5023 – 5029, 2015, doi:10.1109/TIA.2015.2428679

[9] M. Nayel, B. Lu; Y. Tian; Y. Zhao, "Study of Soil Resistivity Measurements in Vertical Two-Layer Soil Model", Proc. of the 2012 Asia-Pacific Power and Energy Engineering Conference, pp. 1-5, 2012, doi:10.1109/APPEEC.2012.6307337

[10] H. Yang, J. Yuan, Y. Zong, "Determination of three-layer earth model from Wenner four-probe test data", IEEE Transaction on Magnetics, vol. 37, no. 5, pp. 3684-3687, 2001, doi:10.1109/20.952690

[11] M. Zhou, J. Wang, L. Cai, Y. Fan, Z. Zheng, "Laboratory Investigations on Factors Affecting Soil Electrical Resistivity and the Measurement", IEEE Transactions on Industry Applications, vol. 51, no. 6, pp. 5358 – 5365, 2015, doi:10.1109/TIA.2015.2465931

[12] D. Stet, L. Czumbil, D.D. Micu, V. Topa, L. Ancas, "Stream Gas Pipeline in Proximity of High Voltage Power Lines. Part I - Soil Resistivity Evaluation", in Proc. of the 47th International Universities' Power Engineering Conference, (UPEC), London, UK, September 4-7, 2012, doi:10.1109/UPEC.2012.6398445

[13] I. F. Gonos; I. A. Stathopulos, "Estimation of multilayer soil parameters using genetic algorithms", IEEE Transactions on Power Delivery, vol. 20, no. 1, pp. 100 - 106, 2005, doi:10.1109/TPWRD.2004.836833

[14] H. Eroglu, M. Aydin, "Genetic algorithm in Electrical Transmission Lines path finding problems", in Proc. of the 8th International Conference on Electrical and Electronics Engineering, (ELECO), Bursa, Turkey, November 28-30, 2013, doi:10.1109/ELECO.2013.6713814

[15] G. Gilbert, Y.L. Chow, D.E. Bouchard, M.M.A. Salama, "Soil model determination using asymptotic approximations to Sunde's curves", in Proc. of the 2010 IEEE PES Transmission and Distribution Conference and Exposition, New Orleans, USA, April 19-22, 2010. doi:10.1109/TDC.2010.5484199

[16] W.P. Calixto, A.P. Coimbra, J.P. Molin, A. Cardoso, L.M. Neto, "3-D Soil Stratification Methodology for Geoelectrical Prospection", IEEE Transaction on Power Delivery, vol. 27, no. 3, pp. 1636-1643, 2012, doi:10.1109/TPWRD.2012.2193602

[17] A.C.B. Alves, R.P. Marinho, G.A.A. Brigatto, L.P. Garces, "Multilayer Stratification Earth by Kernel Function and Quasi-Newton Method", IEEE Latin America Transactions, vol. 14, no. 1, pp. 225-234, 2016. doi:10.1109/TLA.2016.7430083

[18] W. R. Pereira, M. G. Soares, L. M. Neto, "Horizontal Multilayer Soil Parameter Estimation Through Differential Evolution", IEEE Transactions on Power Delivery, vol. 31, no. 2, pp. 622-629, 2016, doi:10.1109/TPWRD.2015.2475637

[19] R.L. Haupt, D.H. Wernwr, Genetic Algorithms in Electromagnetics, Ed. IEEE Press, Wiley-Interscience, pp. 5-290, 2007

[20] Y. Song, Z. Bi, K. Liu, "Method for Soil Resistivity Measurement Based on Neural Network", Proc. of the Third International Conference on Natural Computation (ICNC 2007), vol. 3, pp. 301-305, 2007, doi:10.1109/ICNC.2007.470